Appl. Phys. B 61, 73–80 (1995)

Applied Physics B Lasers and Optics

SBS mirrors for XeCl lasers with a broad spectrum

H.J. Eichler[1], R. König[2], H.-J. Pätzold[2], J. Schwartz[1]

[1] Technische Universität Berlin, Optisches Institut P11, Strasse des 17. Juni 135, D-10623 Berlin, Germany
(Fax: +49-30/314-26888, E-mail:SCHWARTZ@physik.tu-berlin.de)
[2] Max-Born-Institut für Nichtlineare Optik und Kurzzeitspektroskopie, Rudower Chaussee 6, D-12474 Berlin, Germany
(Fax: +49-30/6392-1229, E-mail:PAETZOLD@mbi.wtza-berlin.de)

Received: 31 March 1994/Accepted: 8 September 1994

Abstract. The stimulated Brillouin scattering threshold of focused broad-band XeCl laser radiation depends on the ratio of the coherence length to the Rayleigh range, which is affected by the transverse beam quality. With reduction of the focal length, the threshold decreases first and then reaches a nearly constant value. In addition, the energy reflectivity is increased. On the other hand, pulse shortening occurs and the phase conjugation fidelity is decreased. Separation of single lines from the structured XeCl laser spectrum improves the SBS efficiency.

PACS: 42.65; 42.60. Da

Phase-conjugating mirrors (PCM) based on stimulated Brillouin scattering (SBS) have been applied successfully to achieve good beam quality from infrared solid-state lasers with high average power [1]. During the last few years considerable efforts have been made to use PCMs also for one of the most important UV laser sources: the XeCl-excimer laser [2–13]. There are some difficulties in this matter because without strong modifications the XeCl laser delivers a spatially inhomogeneous output with low transverse and temporal coherence. Additional complications are caused by the laser spectrum which consists of 4 broad lines [12].

The influence of a broad-band pump laser on the SBS process and the resulting backscattered spectrum have been the subject of several theoretical and experimental investigations. Overviews are given, e.g., in [14, 15]. In summary, a simple narrow-band and stationary description is possible if the pump laser is temporally coherent during the lifetime of the acoustic grating. The transition of broad-band SBS is usually defined by a laser bandwidth larger than the Brillouin linewidth of the SBS medium. This corresponds to a laser coherence time smaller than the phonon lifetime.

In the broad-band case it has to be distinguished if the pump laser coherence length is smaller or larger than the SBS interaction length l_i (which is related to the Rayleigh range in focusing geometries). If the pump laser is coherent over the complete interaction range, the narrow-band description applies, otherwise deviations from this description are noticeable [16]. Until now, most broad-band experiments have been performed in a regime where a narrow-band description is possible. According to Narum et al. [17] different longitudinal laser modes separated by a frequency larger than the Brillouin line-width of the medium (this is in the range of GHz for liquids) can be scattered from each other's phase gratings. For that, the coherence length l_c has to exceed the gain length in order to disregard the phase mismatch between different modes.

In an another experiment, SBS with different laser lines has been investigated using a 2500 nm HF laser. 31 lines are distributed over 640 nm. This emission was focused both into a single volume and also spectrally dispersed before focusing [15]. Reflectivity and phase-conjugate fidelity were shown to be equal in both cases and the values were as expected from single line experiments. The coherence length of line pairs was in the range of 1–5 mm, whereas l_c of the individual lines exceeded 80 cm. The 'characteristic gain length' was below 1 cm.

Without narrowing the 308 nm XeCl laser, its output frequency spreads over more than 1200 GHz (0.5 nm) subdivided into two stronger (0–1 and 0–2) and two weaker transitions (0–0 and 0–3) [8, 11–13]. Longitudinal modes do not become evident. In contrast to the HF laser, the individual transitional lines are not very coherent, their linewidth is in the range of 100 GHz.

O'Key and Osborne investigated bandwidth and spatial beam-quality limitations for SBS using the XeCl laser [11]. Either a 616 nm dye laser with 2.5 GHz bandwidth and frequency doubling or a free-running XeCl oscillator with modified spatial beam structure were used as master oscillators with a good beam quality and different bandwidth. Both were XeCl amplified; after that, the broad-band laser divergence was variable between 2 and 50 times diffraction limited. In this experiment the so-called 'SBS threshold' and the saturation reflectivity scale with the interaction length and the focus diameter, which have been varied via bandwidth and beam divergence.

Other spatial beam properties were not considered. If a relatively low divergence (2.5 times diffraction limited) is chosen, the narrow-band pump beam resulted in a saturation reflectivity nearly equal to the full spectrum pump.

An opposite result was obtained recently by Perrone and Yao [13]. A XeCl oscillator was spatially filtered, spectrally narrowed to select the 0–1 transition ($\Delta\nu = 130$ GHz) and power amplified for output energies sufficient for SBS experiments. Using this laser, SBS backscattering could be observed with less than 0.2 mJ pump energy, reaching a saturation level of 30% energy reflectivity at higher pump energies. Although the linewidth reduction was much weaker than in [11], there was an obvious difference to the full spectrum pump, where equal thresholds but only 15% maximum reflectivity have been found.

The inconsistent results of [11] and [13] require further experiments, as will be described in the following. It is investigated to what extent the performance of PCMs for excimer lasers is influenced by the structured spectrum. This is done with a simple single-stage laser with only weak transverse-mode discrimination. Nevertheless, the spatial beam characteristics were held as constant as possible when varying the bandwidth because they can strongly influence SBS results [18]. The large number of oscillating modes and the discharge properties lead to complicated spatial, spectral and temporal details which are difficult to determine accurately.

In order to achieve efficient SBS pumped by broad-band lasers strong focusing is required [19]. As will be shown in Sect. 2, this results in a short interaction range in which the pump beam is coherent. In the following section the achievement of high maximum reflectivities will be discussed.

Strong focusing leads to high intensities in the focal region so that additional nonlinear effects become possible [20]. Therefore, a decrease of phase-conjugation fidelity and transverse coherence in the back-scattered signal can be expected. So, Sect. 4 deals with consequences of strong focusing.

1 Experiment

A commercial excimer laser head (Lambda Physik®, EMG 1003i type) was used as the pump source for the following backscattering experiments. The line-width of the XeCl laser can be narrowed by a grating in the laser resonator (Littrow arrangement, 2100 lines per mm). This reduces the emission to one of the XeCl-laser transitions with weak narrowing to $\Delta\nu = 60$ GHz.

For SBS experiments using the radiation of unmodified single-stage XeCl lasers it is essential to cut away more divergent outer parts of the beam cross section [7]. In the present setup, a 5 mm diameter aperture was placed inside the cavity, this also leads to good performance of the grating used for frequency narrowing in the cavity. In addition, a 7 mm diaphragm was arranged in front of the SBS cell.

For comparable beam polarizations, the XeCl laser was operated without the Littrow grating for frequency narrowing but with an intracavity polarizer. Thus, the lasers with and without frequency narrowing have a comparable degree of polarization: 0.96 and 0.95. The temporal pulse shapes have an equal FWHM duration of 11 ns. The two-dimensional beam shape and the half-angle beam divergence Θ of both lasers are comparable ($\Theta = 0.75 \times 0.80$ mrad). The polarized laser without grating delivers an output energy of up to 25 mJ, which was reduced by about 40% by selection of one transition.

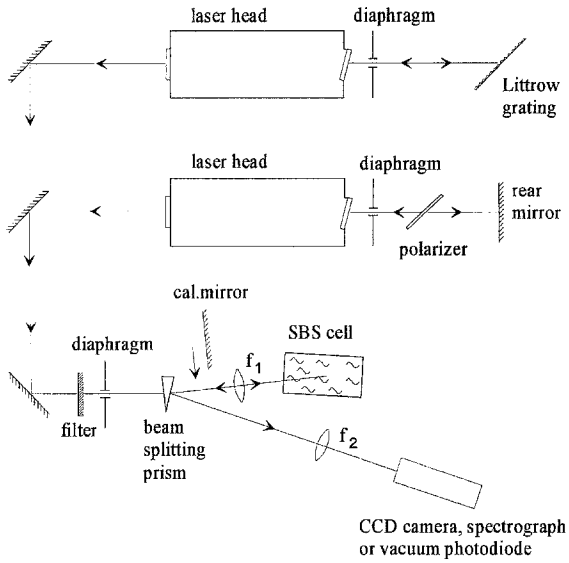

Fig. 1. Experimental setup. Grating and broad-band resonator variants (*upper*) and SBS backscattering arrangement (*lower*)

For SBS investigations, a typical setup is used (Fig. 1, lower), described in detail earlier [7]. The pump-laser radiation is focused into the liquid or gaseous SBS material by means of a fused-quartz lens. The backscattered signal is coupled out from a wedge and detected by a vacuum photo-diode, CCD beam-profiler or spectrum analyzer.

The spectral beam characteristics of the pump laser and the SBS signal are checked by a 2.5 m grating spectrograph. The spectra are read out by a CCD array, accumulated over 100 shots. The divergence is determined using a special CCD beam-profiler for excimer lasers [21].

The transversal coherence is determined by the Young's double slit method. A slit distance with a 0.5 modulation depth of the interference pattern is assumed as the transversal coherence length [22].

All investigated liquids are of high chemical purity (UV spectroscopy grade) because earlier low absorption has been shown to be essential [23].

2 Spectral influences on the reflectivity threshold

The efficiency of backscattering is investigated by using the broad-band laser source, in addition with single-line pumping for comparison. The reflectivity is defined by the ratio of pulse energies here. Usually, the dependence of the reflectivity vs pump energy is largely characterized by two

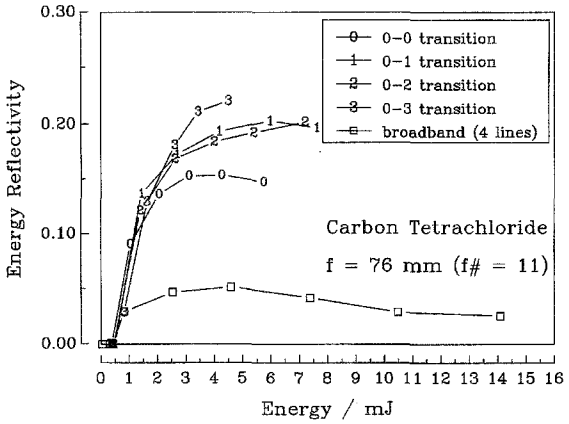

Fig. 2. Energy reflectivity of carbon tetrachloride as a function of the pump energy for different lines. The behavior of the broad-band laser is depicted also

parameters: the threshold pump energy and the saturated reflectivity.

Supporting the results of [13], Fig. 2 shows a large difference in the saturated reflectivity between broad-band and narrow-band pumping. The broad-band laser beam is less reflected than the single-line pump laser. This can be observed using different materials and focusing lenses. The results for the different single lines do not differ so much. The weaker lines show small deviations without regularity. So, in the following, the different narrowed lines are assumed to give equal results. In Fig. 2 another interesting fact should be noted: there is no obvious difference in the threshold energies between broad-band and single-transition pumping.

It shall be investigated now whether the threshold is influenced by line narrowing for different focal lengths. Apart from its practical importance, the SBS threshold is a favourable parameter for the interpretation of the back-scattering effect. In principle, it is given by the energy or intensity resulting in significant amplified backscattering exceeding noise. Experimentally, the threshold energy E_{th} can be defined as the value, where an energy reflectivity of $R_E = 2\%$ (or 5% percent power reflectivity) is observed. Such values are depicted in Fig. 3 as a function of the focal length.

Although the diagrams Fig. 3a–c differ in the used SBS liquids—i.e, especially in the Brillouin gain coefficient g—all curves can be divided into two regions: up to a certain focal length of about $f = 80$ mm, the threshold is approximately constant, pumping with one as well as with all lines led to nearly equal results in the constant region. Larger focal lengths increase the threshold energy. The threshold grows slower if the pump beam is more coherent. In principle, this behaviour agrees with previous results obtained with a better-beam-quality Nd:YAG laser [24].

All our experiments are *broad band* because the pump-laser radiation becomes incoherent during the interaction with a phonon which has a lifetime τ_B, i.e., $l_c < c\tau_B$ (c: light velocity in the medium) [25]. Even with the grating resonator, the laser bandwidth ($\Delta\nu \geq 60$ GHz) is always far above the Brillouin line width

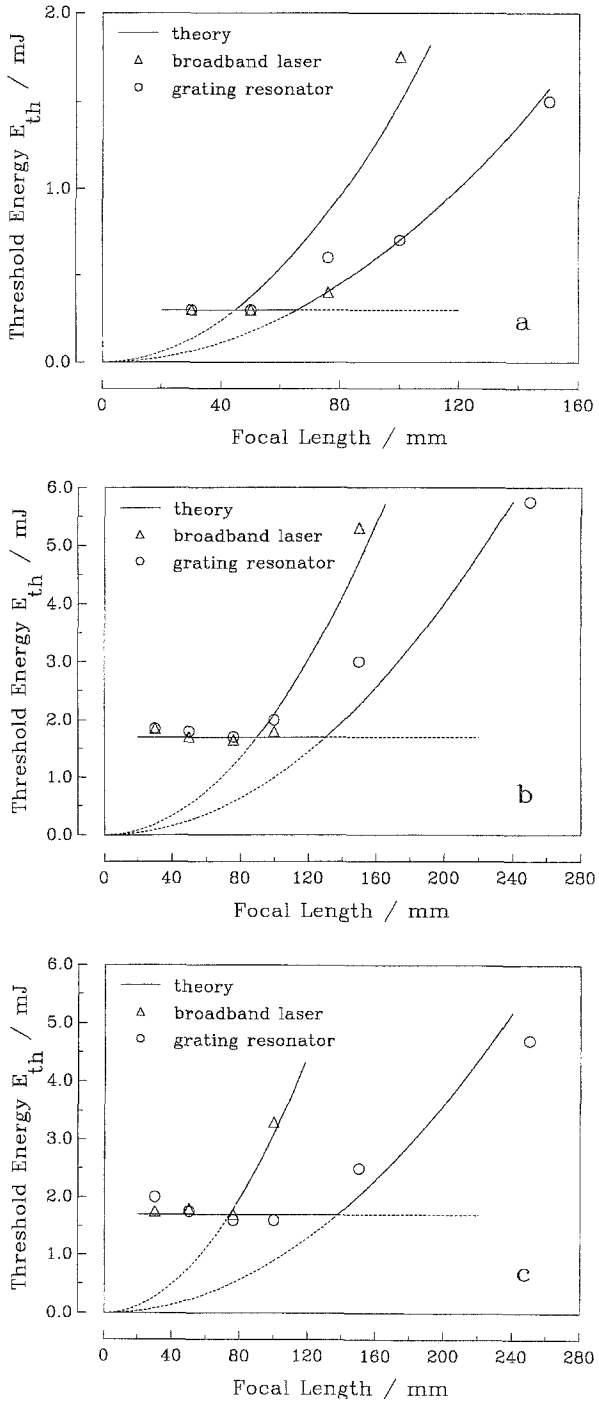

Fig. 3a–c. SBS threshold energy vs focal length. Broad-band and line narrowed pump conditions are compared for carbon tetrachloride (**a**), n-hexane (**b**) and cyclohexane (**c**). The focal length variation $f = 30$–250 mm corresponds to a range of the f number f/d between 4.3 and 35

($\delta\nu_B = 1$–4 GHz, i.e., $\tau_B = (2\pi\delta\nu_B)^{-1} = 40$–$140$ ps [26]). Nevertheless, the narrow-band model can be applied in this case if the pump wave is coherent in the region of interaction, i.e., $l_c > l_i$.

In common SBS models, the threshold is defined by an intensity I_{th} required to get a certain value of amplification exponent G, where the backscattered signal exceeds the noise (usually $G = 20$–30). Although in the UV, the

phonon lifetimes are small with respect to the laser-pulse duration t_p, transient behaviour has to be considered. So the threshold condition can be written as [7]

$$\frac{gI_{th}l_i t_p}{\tau_B} = G^2 \approx 600. \tag{1}$$

Using the threshold pulse energy E_{th} and the cross-section area of the focused spot $A = \pi w_0^2$ one can also write

$$\frac{gE_{th}l_i}{A\tau_B} = G^2. \tag{1a}$$

In (1a), l_i is most relevant. Two cases can be classified:
1) If $l_c > l_i$, the interaction length l_i is determined by the strength of focusing. l_i has been found to be proportional to the Rayleigh range z_R of the focused beam: $l_i = mz_R$, (e.g. $m = 5$ for special experimental conditions [27]). The Rayleigh range depends on the laser wavelength λ and on the focal length. The factor M^2 has to be added for non-Gaussian beams [28]:

$$l_i \propto z_R = \frac{\pi w_0^2}{\lambda M^2}$$

$$\text{with } w_0 = \frac{f\lambda M^2}{\pi d}. \tag{2}$$

Here, d gives the spot size incident before the lens. Equations (1) and (2) lead to a threshold energy which is not dependent on the focal length:

$$E_{th} = \frac{G^2 \pi w_0^2 \tau_B \lambda M^2}{gm\pi w_0^2}. \tag{3}$$

2) In the second situation ($l_c < l_i$), the pump beam is focused less strong. So the coherence length l_c has to be assumed as the real interaction length [25], because only within this range coherent interaction occurs. So (1) results in increasing E_{th} with the focal length:

$$E_{th} = \frac{G^2 \pi w_0^2 \tau_B}{gl_c} = \frac{G^2 \tau_B \lambda^2}{gl_c \pi d^2} f^2. \tag{4}$$

The thresholds of broad-band and narrow-band pumped SBS are equal using short focal lengths. This is because the narrow-band model is applicable independent of the laser bandwidth if $l_c > l_i$ is fulfilled. So, in (3), g keeps its narrow-band value, probably reduced by spatial effects [14]. However, the laser bandwidth influences the threshold energy if $l_c < l_i$:

From (4), a quadratic dependence of the threshold from the focal length can be expected. This is confirmed by the experimental results shown in Fig. 3. The f^2 curves have been fitted to the experimental data by using two different values for l_c, one for the broad-band pump and the other for the line-narrowed laser.

The increased threshold at long focal lengths has also been seen in spectral investigations. Figure 4 shows a comparison of the backscattered-radiation spectrum in the cases of very strong ($f = 20$ mm) and weaker focusing into the SBS medium ($f = 100$ mm). It should be noted

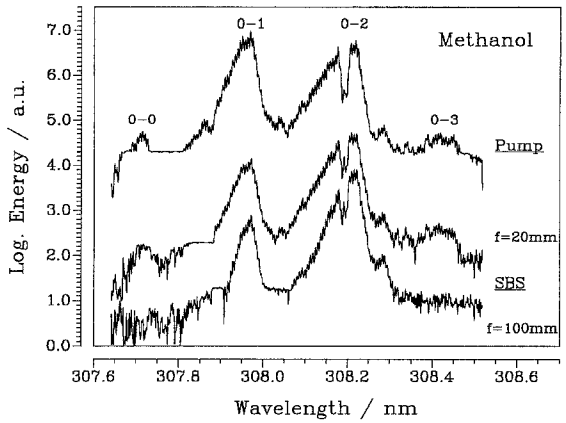

Fig. 4. Spectrum of the XeCl pump laser, observed by means of a 2.5 m grating spectrometer. The spectra after SBS reflection using strong ($f = 20$ mm) and weaker focusing ($f = 100$ mm) differ in the appearance of the weaker lines

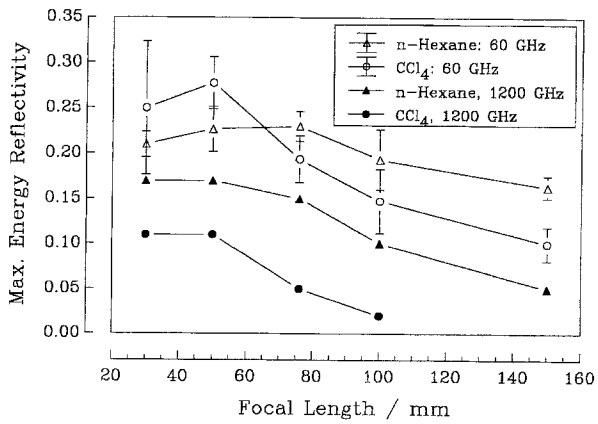

Fig. 5. Focal-length dependence of the maximum energy reflectivity for unnarrowed and single-line pumping. The values are obtained at a constant pump energy of about 5 mJ. The choice of this energy is justified by the results presented in Fig. 8. The *bars* indicate the deviation obtained for the different single lines

that the weaker 0–0 and 0–3 transitions appear in the SBS reflection spectrum at $f = 20$ mm only. They seem to reach the threshold individually at very high intensities only. Similar reflection spectra have been observed with different SBS liquids which have different gain values.

3 Maximum reflectivity

Carbon tetrachloride is an interesting SBS material because it has a very low threshold energy. But hexane has been shown to give a larger reflectivity with broad-band XeCl laser radiation [7]. Measured maximum energy reflectivity values with and without spectral narrowing are depicted in Fig. 5. They depend on the scattering material and on the strength of focusing. Similar to the threshold behavior, there is a noticeable difference between multi- and single-line pumping. With line narrowing and strong focusing the reflectivity of CCl_4 becomes comparable or better than that of *n*-hexane.

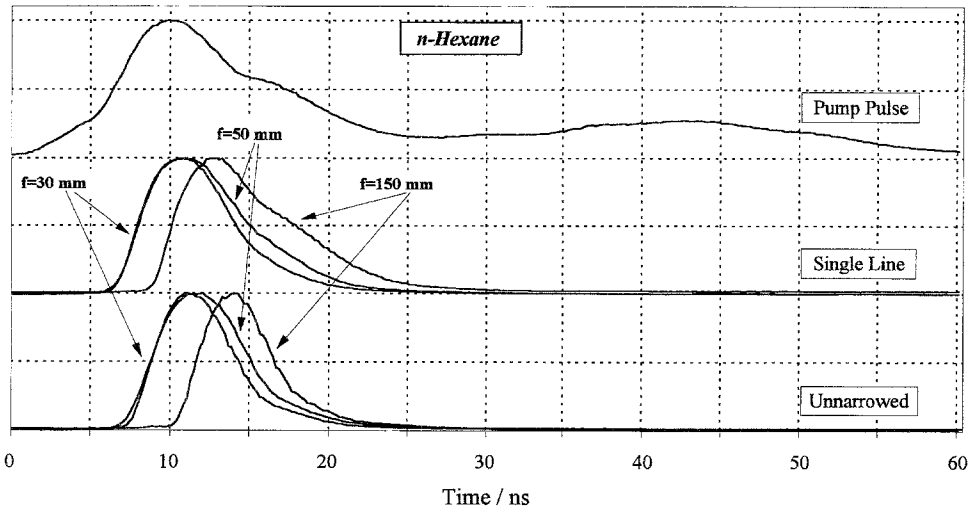

Fig. 6. Temporal behavior of the reflected power under different focusing conditions. Results using the line narrowed laser are compared with those obtained by the complete broad-band spectrum. The pulse intensities are shown in normalized units

Theoretically, the behavior of reflectivity vs pump energy in the saturated region is less well understood for broad-band pumped SBS [14]. A look on the temporal development of the backscattered pulses can be helpful to understand the experimental results. In Fig. 6, the shapes of the reflected pulses are compared under different linewidth and focusing conditions. Typical results for *n*-hexane are exhibited. Each pulse intensity is scaled relative to its peak value.

As noticeable from Fig. 6, there is a small pulse compression at $f = 50$ mm and single line operation, i.e., the reflected power increases with minimum delay and has a comparably long duration. Independent of the pump linewidth, the pulse shortening is increased if very short focal lengths ($f = 30$ mm) are used. On the other hand, the pump-pulse leading edge is not reproduced using weak focusing ($f = 150$ mm). The backscattered pulse is shifted to the less intensive rear part of the pump pulse where SBS amplification is smaller. In any case, the application of the broad-band laser leads to a more delayed start of the backscattered signal, i.e., all SBS pulses are shorter here.

A comparison of Figs. 6 and 3 indicates that there is a correlation between the threshold energy and the delay time of backscattering. Short focal lengths result in a low threshold energy and lead to an early rise of the SBS signal. But, in the region of increased thresholds, i.e., $f > 80$ mm, there is an increased delay. As expected from the above model, this effect is amplified by a larger linewidth.

The pulse-shortening effects are summarized in the ratio of input and backscattered pulse durations for a broad-band pump. This ratio is shown in Fig. 7 as a function of the focal length for liquid and gaseous SBS samples. It is obvious that the pulses are strongly shortened using long focal lengths as well as $f = 30$ mm. In the first case, according to Fig. 6, the reflectivity has a late start and decreases together with the pump-pulse power. Stronger focusing leads to a nearly instantaneous start of backscattering. The amplification is high at the leading

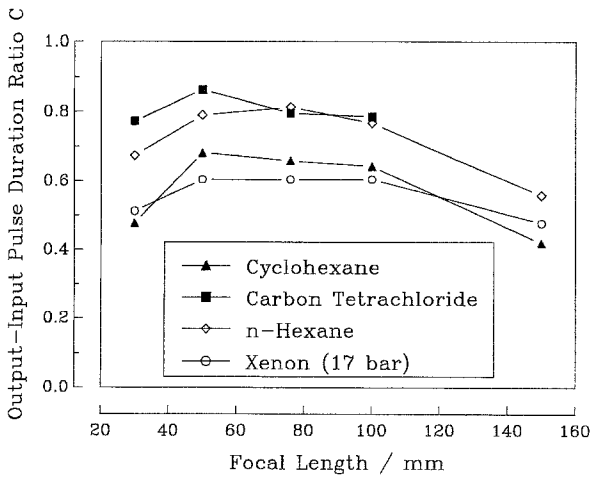

Fig. 7. Ratio of SBS pulse duration and pump pulse duration (FWHM) plotted as a function of the focal length. The values are derived at about 5 mJ pump energy for a broad-band pump

edge of the pump pulse but the reflectivity is interrupted soon for very short focal lengths. This temporal behavior is consistent with the non-increasing values of the maximum energy reflectivity for short focal lengths in Fig. 5.

Possible reasons for this pulse-shortening phenomenon for high intensities are thermal effects, because we observe no bandwidth dependence. Thermal interactions with SBS are induced by refractive-index changes due to light absorption and may become effective in different ways:

1) A temperature modulation along the light-propagation path leads to Stimulated Thermal Scattering (STS).

2) Transient variations of the refractive index n in the interaction region result in phase changes of the pump and the Stokes wave and, therefore, modify the spectrum of the backscattered radiation [29].

3) Transverse changes of n during the pulse can result in thermal self-defocusing [30].

In contrast to SBS, scattering from a temperature grating gives a negligible frequency shift between pump and backscattered radiation [20, 31]. We checked this for our conditions and did not observe an unshifted STS contribution in the reflected radiation spectrum. The output of the line-narrowed laser was focused strongly ($f = 20$ mm) into cyclohexane. By means of the 2.5 m grating spectrograph, a shift of $\delta\lambda = 2$ pm, i.e., $\delta\nu = 6$ GHz was found. The calculated value amounts to 12.5 GHz obtainable from literature data [26, 32]. The fact that the measured shift is smaller than the calculated Brillouin frequency shift is consistent with other backscattering experiments using different liquids, e.g., n-hexane [20].

Such a reduced Brillouin shift may be caused by thermally induced refractive-index changes in the focal region [29]. In the used low-absorbing media (linear absorption coefficient $\alpha = 0.01$–$0.1\ \mathrm{cm}^{-1}$), this effect becomes evident for sufficiently long pulses only [33]. Only in this case, a laser-induced acoustic pressure wave has enough time to propagate across the beam radius w_0 during the pulse [29, 30]. For the pulse duration t_p this means

$$t_p \geq \frac{f\lambda M^2}{\pi d v_s}, \tag{5}$$

where v_s is the sound velocity. For the present parameters, the condition (5) is fulfilled for short focal lengths ($f < 50$ mm).

After the characteristic time w_0/v_s thermally induced refractive-index changes build up which may have two effects on SBS: either there can be self-induced change in the pump and Stokes frequency [29, 33] or thermal self-defocusing of the pump can occur [30, 34]. The first process alters the spread of the grating formed by the acoustic wave. As a result, transient broadening of the backscattered spectrum will occur. Such an increase of the bandwidth of the backscattered radiation by 150 MHz using CCl_4 and a ruby laser has been found experimentally in ref [33]. We estimated that in our experiment a temperature rise of 1 K results in a frequency broadening of about 100 MHz. When the broadening comes near to the SBS linewdith (e.g., 520 MHz for CCl_4 and $\lambda = 694$ nm [26]), the effectiveness of the SBS process is reduced. This is possible reason for the premature interruption of the backscattered pulses observed for short focal lengths ($f = 30$ mm in Fig. 6). Condition (5) is fulfilled here and the heat load per unit volume is particularly high.

Apart from frequency broadening of the backscattered radiation, self-induced refractive-index changes can also result in defocusing of the pump beam in the interaction region [30, 34]. Due to that, the peak pump intensity falls and, as a consequence, also the reflected signal is attenuated. The degree of defocusing is proportional to the pump energy, so the occurrence of this effect is supported by the decrease of SBS reflectivity at high pump energies shown in Fig. 8.

Due to the low threshold energy value of carbon tetrachloride, a pump energy of 50 times the threshold was reached in that experiment. In this region, we observe

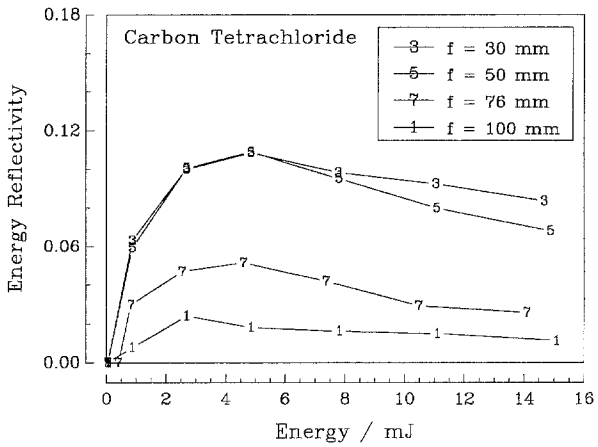

Fig. 8. Energy reflectivity of carbon tetrachloride vs pulse energy of the broad-band pump laser using lenses of different focal length

a reflectivity decrease in Fig. 8. A reflectivity decrease using high pump intensities has been reported earlier [9]. Filippo and Perrone explained it by the onset of other nonlinear effects due to high intensities. In contrast to that, we observed a similar decrease for all focal lengths. This supports the assumption that the reflectivity decrease is caused by thermal defocusing which depends on the pump energy and not on the intensity [34].

A similar dependence on the pump energy has been observed concerning the quality of wave-front reconstruction of the pump beam [35]. There, thermal effects are cited as possible explanations, too. In general, a negative influence on the so-called fidelity has been found for all thermal effects discussed above [22, 29, 34]. According to (5), the occurrence of thermal effects is more likely at short focal lengths. Therefore, in the following, we investigated the influence of strong focusing on the phase-conjugating properties.

4 Beam reconstruction and fidelity

One of the main reasons for practical interest in SBS is its wave-front reversal property. It is usually quantified by means of a "fidelity" parameter, which denotes the fraction of the backscattered signal exactly conjugated to the incident wave. The measurement requires the separation of conjugated and non-conjugated backscattered energy (or power). This can be realized by a double pass through a diffuser with intermediate SBS [36, 37]. Alternatively, a controlled phase shift can be induced by a diffraction grating [38] or by heterodyning two SBS-PCMs having a different Brillouin shift [39]. All these techniques work best with diffraction-limited beams or plane waves, which are often not easily available. For this reason, a more pragmatic procedure referred to as the "fidelity in terms of divergence" has been introduced, which is useful for excimer lasers. This "far-field fidelity" is related to the angular distribution of the SBS beam and may have values above unity. It can be measured by the "energy-in-the-bucket-technique" [35] or by comparing the divergence of SBS and pump beam [13].

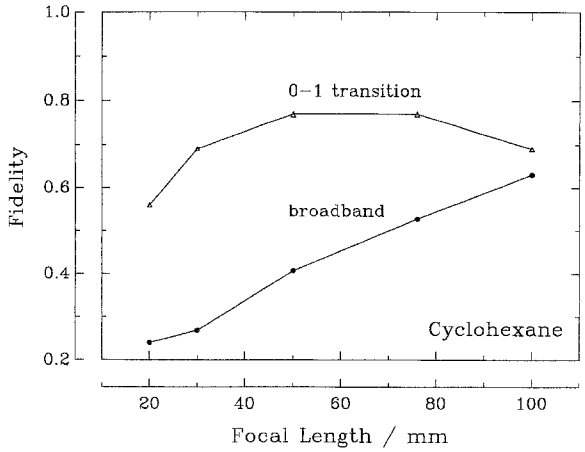

Fig. 9. Fidelity in terms of divergence as a function of focusing into a cyclohexane SBS cell. Two cases are compared: Pump with the complete laser spectrum and narrowed to a single line (0–1 transition, $\Delta\lambda = 15$ pm)

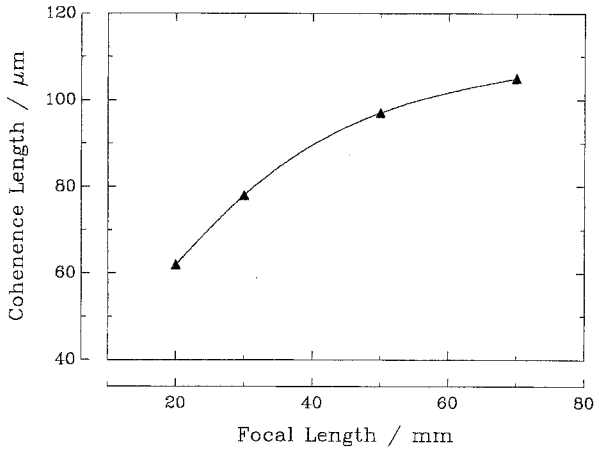

Fig. 10. Transversal coherence of the radiation backscattered from carbon tetrachloride. The focal length was varied at a constant broad-band pump energy of 5.2 mJ

The ratio of SBS-beam divergence to pump-beam divergence, i.e., the fidelity in terms of divergence, is depicted in Fig. 9 as a function of the SBS-lens focal length. The divergence values are derived from beam profiles in the focal plane of a long-focus lens ($f = 4.4$ m). The beam diameters have been derived at the level of half-maximum energy in the direction perpendicular to the discharge. It turns out that the fidelity with the broad-band pumping is increasing with the focal length. On the other hand, if the spectrum is narrowed to a single line (e.g., the 0–1 transition), only very short focal lengths lead to a drastic fidelity decrease.

In this context, transverse coherence measurements indicate that not only the divergence but also other beam properties are reproduced worse using short focal lengths. This has been measured using the broad-band laser. The initial transverse coherence length of the output is about 110 µm. As shown in Fig. 10, it decreases similarly to the fidelity. The beam looses spatial phase information.

According to Schelonka et al., the fidelity is exclusively determined by the focal intensity [37], which is large for short focal lengths. Using excimer lasers, a deleterious influence of high pump laser energies [13] and intensities on the fidelity has been reported. Also a negative effect of large bandwidths has been found [10, 13]. The dependence of the fidelity on the laser bandwidth of a KrF-excimer laser was investigated systematically by Davis and Gower [40]. A strongly oscillating behavior has been found. This could not be proved by us for the XeCl laser because we checked two bandwidth values only.

In the present experiments, we observed that the shape of the backscattered spot and its intensity are strongly dependent on the adjustment and the quality of the SBS focusing lens, e.g., a non-centric pass of the beam through the lens leads to considerable losses.

So, increased lens aberrations are possible reasons for a decreased fidelity at short focal lengths aside from high-intensity effects. Particularly, chromatic aberration, i.e., a wavelength-dependent focus location, can illustrate the influence of the pump spectrum. It is estimated that the large spectral width of the XeCl laser emission will lead to a spatial dispersion of the focus locations $\Delta f \approx 100$ µm assuming a $f = 100$ mm lens. The coherence length determined from the bandwidth is of the same order of magnitude. This means that the acoustic gratings of the different lines are shifted within a range Δf. The value of Δf is proportional to f. Therefore, different parts of the spectrum are reflected in a narrower range if the focusing is stronger. Long focal lengths lead to spatial dispersion of different focal spots of the laser lines. Then, each is reflected at its own acoustic grating with reduced interaction with other lines resulting in a good fidelity. Similarly, spectral narrowing prevents line interaction and increases the fidelity. This is consistent with our observations.

The fidelity decreases at very short focal length for both investigated bandwidths. The reason for that becomes clearer from the near-field spatial profiles depicted in Fig. 11. The backscattered-radiation profile is strongly deformed if very short focal lengths are used. The appearance of a sharp central maximum indicates that nonlinear effects occur in the focal region.

Self-focusing or defocusing by non-linear refractive-index changes is often cited in this context [9, 40]. These changes lead to spatial broadening of the pump beam in the focus resulting in a backscattered beam with smaller cross section at the output [34]. On the other hand, we observed constriction of the beam in the waist region inside the SBS cell for very strong focusing ($f = 20$ mm). Furthermore, a more rectangular beam profile (see upper part of Fig. 11) is not advantageous for self-focusing phenomena. So, probably, the observed peak is a result of small-scale self-interaction of the irregular transverse beam profile of the excimer laser.

5 Conclusion

The SBS threshold is a convenient parameter for the theoretical treatment of SBS. This also holds true in the case of single-stage XeCl excimer lasers. In order to achieve low threshold energies together with high energy reflectivities, the focal length has to fall below a certain value (the transition point between constant and

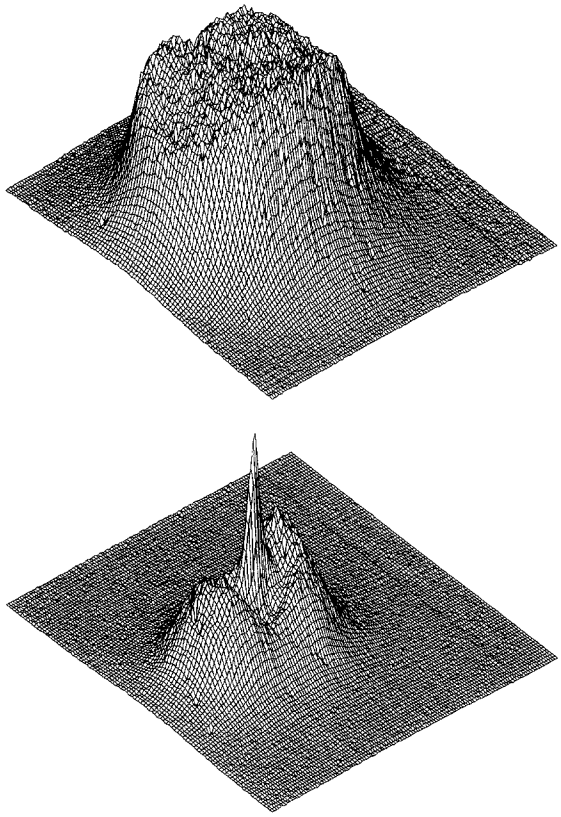

Fig. 11. Near-field spatial beam profiles of the pump laser (*upper*) and the backscattered radiation (*lower*) after very strong focusing ($f = 20$ mm, unnarrowed, focal intensity $I \approx 10^{11}$ W/cm^2)

quadratic dependence in Fig. 3). This has been shown using unmodified XeCl lasers. On the other hand, extremely short focal lengths are disadvantageous for the reconstruction of the broad-band pump-beam properties, i.e., for phase conjugation. Experimentally, this leads to a reduced divergence fidelity and transverse coherence of the reflected beam. The reproduction after SBS backscattering is more satisfying if weaker focusing is used. From these results an optimum SBS focal length for unnarrowed XeCl laser radiation can be found. Using cyclohexane, it is in the range of $f = 50$–70 mm for the conditions investigated.

The SBS backscattering of unmodified multi-line XeCl laser radiation from carbon tetrachloride gives an energy reflectivity of $R_E = 10\%$ and a threshold energy of $E_{th} = 0.3$ mJ. The backscattered pulse duration was 0.9 times the incident FWHM (full-width at half-maximum) and the fidelity in terms of divergence was 0.5.

These reflectivity and fidelity results can be improved considerably by narrowing the structured laser spectrum, i.e., by selection of single transitional line. Maximum energy reflectivity of more than 30% together with a fidelity of 0.8 were demonstrated.

Acknowledgements The authors wish to thank D. Berger, A. Haase, A. Kummrow and R. Menzel for stimulating discussions. Financial support from the BMFT and VDI is gratefully acknowledged.

References

1. H.J. Eichler, A. Haase, R. Menzel: Int. J. Nonlin. Opt. Phys. **3**, 339 (1994)
2. E. Armandillo, D. Proch: Opt. Lett. **8**, 523 (1983)
3. E. Armandillo: Opt. Commun. **49**, 198 (1984)
4. M. Sugii, M. Okave, A. Watanabe, K. Sasaki: IEEE J. QE-**24**, 2264 (1988)
5. V.V. Bertsev, A.A. Pastor, P. Yu. Serdobintsev, N.N. Shubin: Opt. Spectrosc. (USSR) **67**, 830 (1989)
6. J.W. Chen, V. Nassisi, M.R. Perrone: Opt. Commun. **79**, 381 (1990)
7. H.J. Eichler, R. König, R. Menzel. H.-J. Pätzold, J. Schwartz: J. Phys. D **25**, 1161 (1992)
8. A.A. Filippo, M.R. Perrone: Appl. Phys. B **55**, 71 (1992)
9. A.A. Filippo, M.R. Perrone: Opt. Commun. **91**, 395 (1992)
10. A.A. Filippo, M.R. Perrone: IEEE J. QE-**28**, 1859 (1992)
11. M.A. O'Key, M.R. Osborne: Opt. Commun. **89**, 269 (1992)
12. H.J. Eichler, R. König, R. Menzel, H.J. Pätzold, J. Schwartz: Int. J. Nonlin. Opt. Phys. **2**, 247 (1993)
13. M.R. Perrone, Y.B. Yao: Tech. Dig. EQEC '93, Vol. 1, 326 (1993), IEEE J. QE-**30**, 1327 (1994)
14. G.C. Valley: IEEE J. QE-**22**, 704 (1986)
15. W.T. Whitney, M.T. Duignan, B.J. Feldman: J. Opt. Soc. Am. B **7**, 2160 (1990)
16. V.I. Popovichev, V.V. Ragul'skii, F.S. Faizullov: JETP Lett. **19**, 196 (1974)
17. P. Narum, M.D. Skeldon, R.W. Boyd: IEEE J. QE-**22**, 2161 (1986)
18. A. Kummrow, Opt. Commun. **96**, 185 (1993)
19. N.A. Kurnit, S.J. Thomas: IEEE J. QE-**25**, 421 (1989)
20. V.B. Karpov, V.V. Korobkin, D.A. Dolgolenko: Sov. J. Quantum Electron. **21**, 1235 (1992); Phys. Lett. A **158**, 350 (1991)
21. K. Mann, A. Hopfmüller: In *Laser Beam Characterization*, ed. by H. Weber, N. Reng, J. Lüdke, P.M. Mejias (Festkörper-Laser-Institut Berlin, Berlin, 1994) pp. 347–358
22. H.-J. Pätzold, A. Rosenfeld, R. König: Investigations of beam properties of an XeCl laser. Emst Abbe Conf., Jena (1989)
23. H.J. Eichler, R. König, R. Menzel, R. Sander, J. Schwartz, H.-J. Pätzold: Int. J. Nonlin. Opt. Phys. **2**, 267 (1993)
24. Y.-S. Kuo, K. Choi, J.K. Mclver: Opt. Commun. **80**, 233 (1991)
25. R.A. Mullen, R.C. Lind, G.C. Valley: Opt. Commun. **63**, 123 (1987)
26. W. Kaiser, M. Maier: In *Laser Handbook*, ed. by F.T. Arecchi, E.O. Schulz-Dubois, Vol. 2 (North-Holland, Amsterdam 1972)
27. J. Munch, R.F. Wuerker, M.J. LeFebvre: Appl. Opt. **28**, 3099 (1989)
28. A.E. Siegman: SPIE Proc. **1224**, 2 (1990)
29. O.L. Antipov: Sov. J. Quantum Electron. **17**, 458 (1987)
30. E.L. Bubis, V.V. Dobrotenko, O.V. Kulagin, G.A. Pasmanik, N.I. Stasyuk, A.A. Shilov: Sov. J. Quantum Electron. **18**, 94 (1988)
31. S.S. Alimpiev, V.S. Bukreev, S.K. Vartapetov, I.A. Veselovskii, V.I. Kusakin, S.V. Likhanskii, A.Z. Obidin: Sov. J. Quantum Electron. **21**, 80 (1991)
32. T.A. Wiggins, R.V. Wick, N.D. Foltz, C.W. Cho, D.H. Rank: J. Opt. Soc. Am. **57**, 661 (1967)
33. G.B. Krivoschekov, M.F. Stupak, I.G. Kobyakov: Sov. J. Quantum Electron. **12**, 883 (1982)
    G.V. Krivoschokov, M.F. Stupak: Opt. Commun. **46**, 237 (1983)
34. E.A. Volkova, V.P. Kandidov: Sov. J. Quantum Electron. **20**, 695 (1990)
35. J.J. Ottusch, D.A. Rockwell: Opties Lett. **16**, 369 (1991)
36. B. Ya. Zel'dovich, N.F. Pilipetkii, V.V. Shkunov: Sov. Phys. Usp. **25**, 713 (1982)
37. L.P. Schelonka, C.M. Clayton: Opt. Lett. **13**, 42 (1988)
38. P. Suni, J. Falk: Opt. Lett. **12**, 838 (1987)
39. M.J. Damzen, M.H.R. Hutchinson: Opt. Lett. **10**, 40 (1985)
40. G.M. Davis, M.C. Gower: IEEE J. QE-**27**, 496 (1991)